Supplemental figures

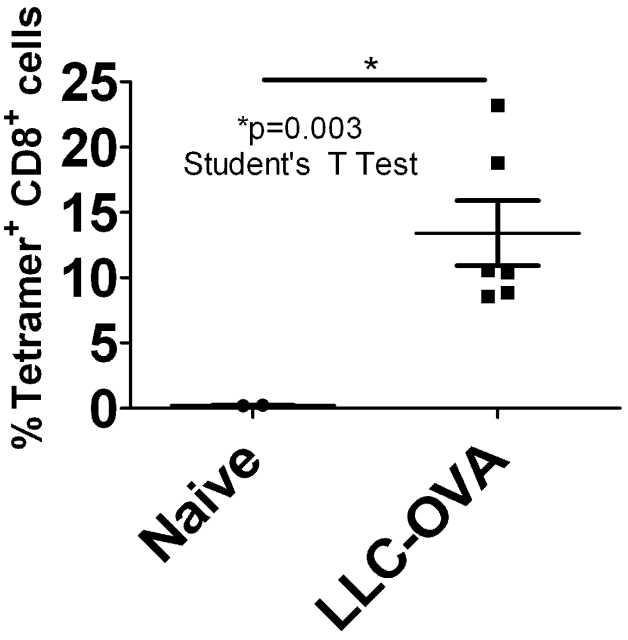

Supplemental Figure 1. Impact of immunogenic-LLC tumors (LLC-OVA) on peripheral OVA-specific CD8 T cells. Tetramer analysis showing percent OVA-specific CD8 T cells in peripheral blood (out of total CD8 T cells) on day 10 from mice receiving LLC-OVA s.c or naïve mice as indicated. Each point represents a single mouse. Student's t test was performed to compare tetramer positive CD8 T cells between naive mice and those receiving LLC-OVA tumors.

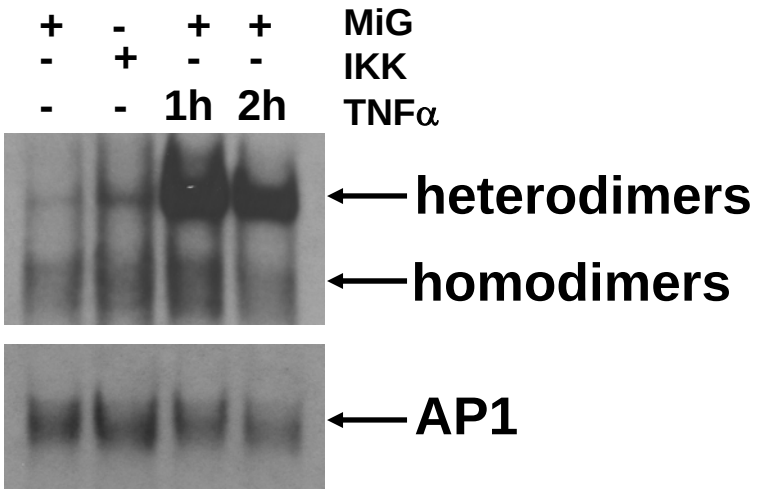

Supplemental Figure 2. Activation of NF-κB in non-immunogenic LLC cells. EMSA showing nuclear levels of NF-κB (top) and AP1 (bottom) in LLC-MiG, LLC-IKK, or LLC-MiG cells treated with TNFα. Results are representative of at least two independent experiments.

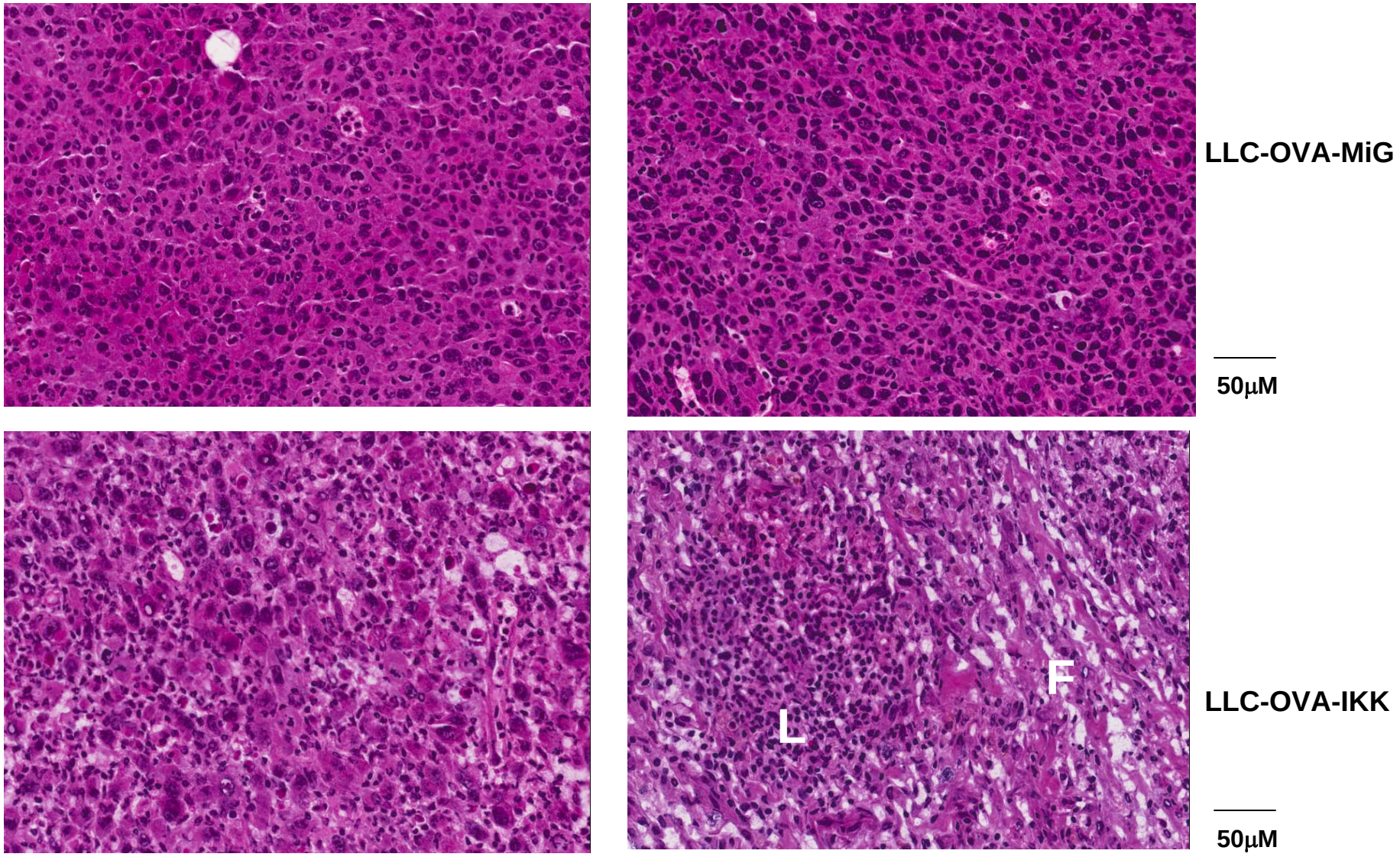

Supplemental Figure 3. (top panel) Two different LLC-OVA-MiG tumors (Day 9) showing a high percentage of neoplastic cells and intra-tumoral infiltrating lymphocytes. (Bottom Panel) Two different LLC-OVA-IKK tumors (Day 10) showing neoplasm and extensive intratumoral lymphocytic infiltration (L) and fibrosis (F).

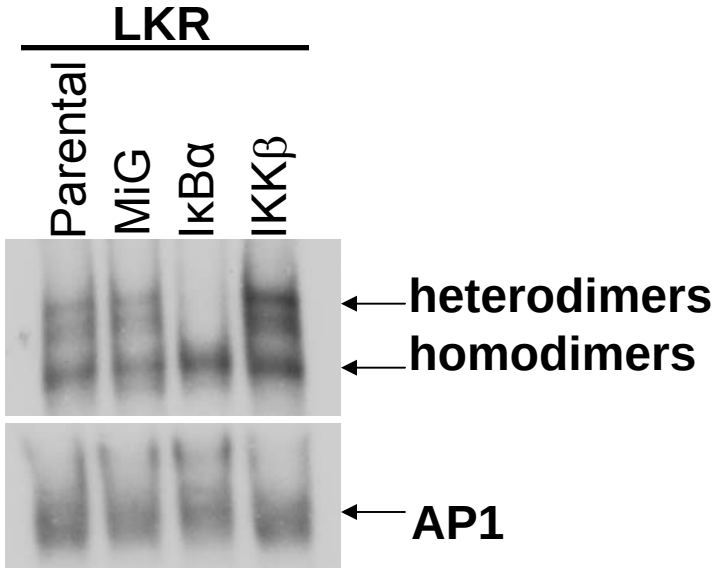

Supplemental Figure 4. NF-κB and AP1 activity as determined by EMSA in parental LKR-13, LKR-13 transduced with the control MiG retrovirus (MiG), IκBαSR retrovirus (IκBα) and CA-IKKβ retrovirus (IKKβ). Mobility of different complexes is indicated with arrows.

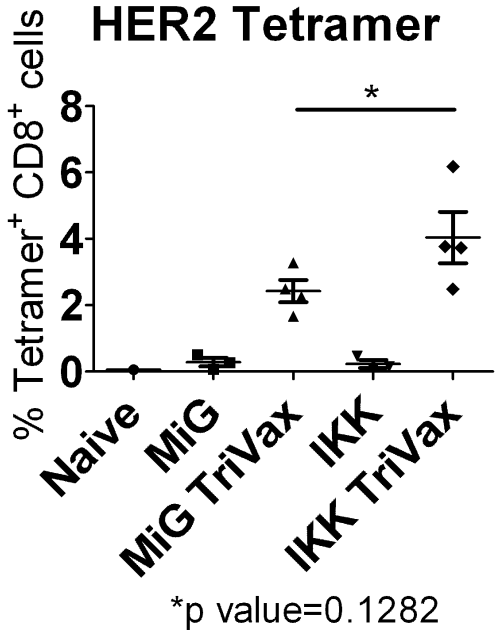

Supplemental Figure 5. Presence of HER2-specific CD8 T cells after TriVax administration. Tetramer analysis of peripheral blood on day 10 from naïve mice or mice receiving TUBO-MiG or TUBO-IKK with or without TriVax vaccination. Vaccination given on day 5. Each point represents data from a single mouse. Results are representative of two independent experiments. Student's T test was performed to compare tetramer positive CD8 T cells between TriVax treated mice receiving TUBO-MiG and those receiving TUBO-IKK tumors.

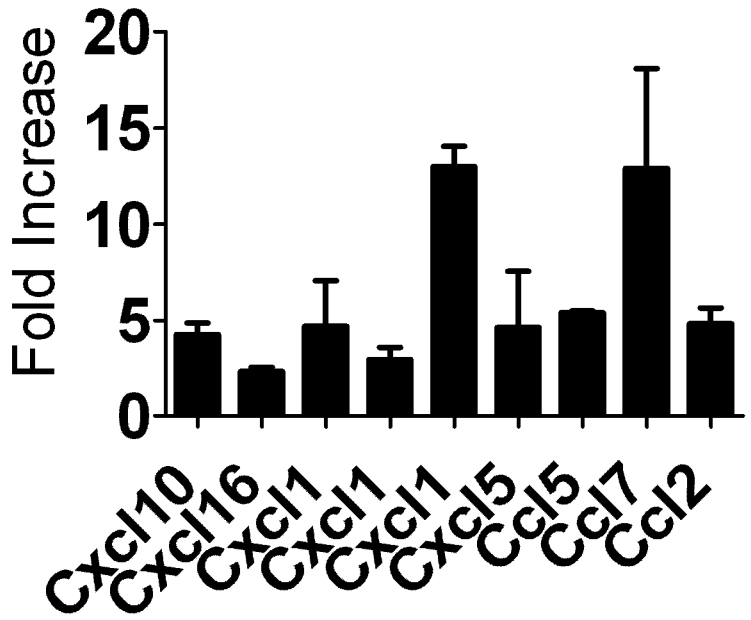

Supplemental Figure 6. Impact of IKKβ expression on chemokine expression in LLC-OVA determined by RNA microarray analysis on an Affymetrix platform. Affymetrix probe set intensity fold increase in indicated chemokine expression in LLC-OVA-IKK compared to LLC-OVA-MiG. Genes identified in two separate microarray experiments are shown, and reported as mean +/- SEM.

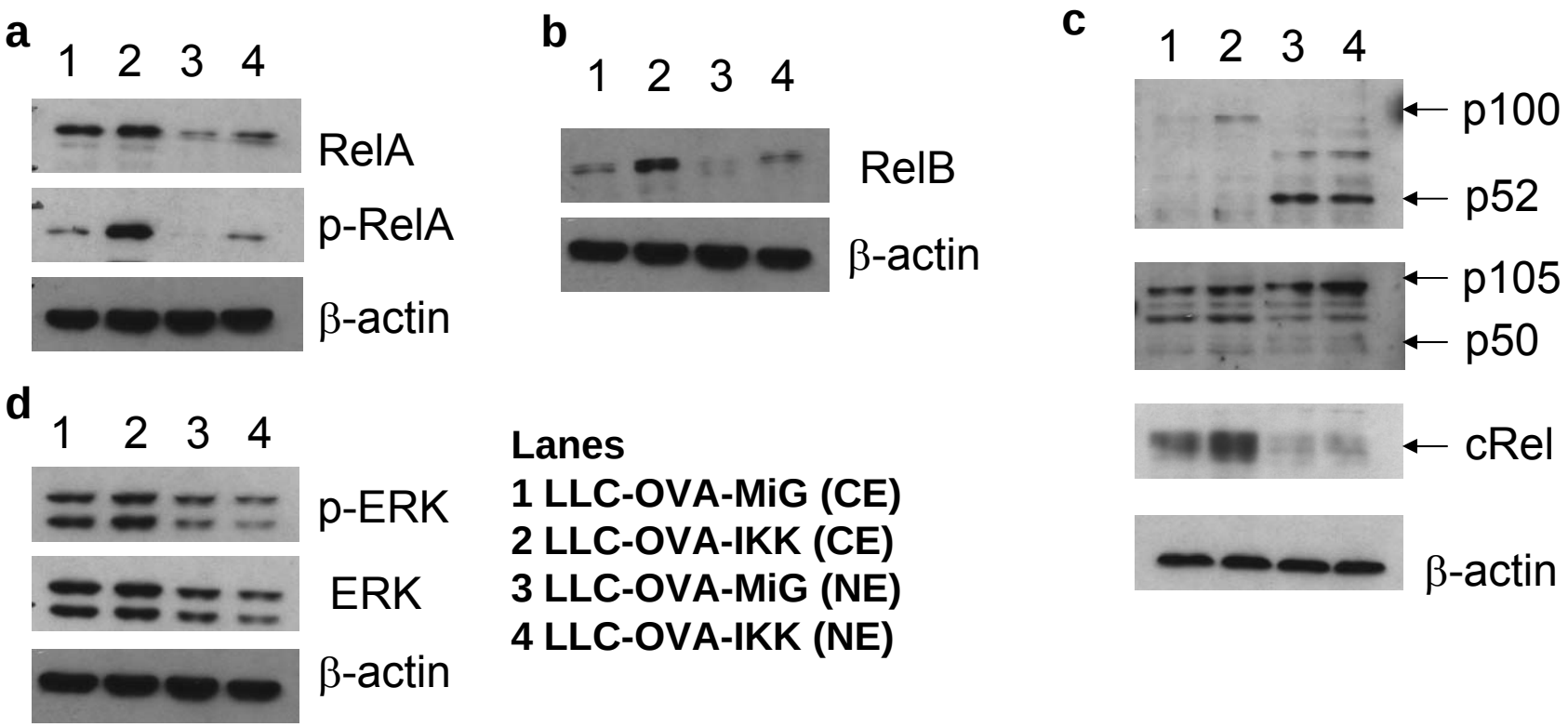

Supplemental Figure 7. (a) Western blot showing RelA and S536 p-RelA in cytoplasmic extracts (CE; lanes 1,2) and nuclear extracts (NE; lanes 3,4) in LLC-OVA-MiG (lanes 1 and 3) and LLC-OVA-IKK (lanes 2 and 4). (b) Western blot of RelB shown as in "a". Western blot of p100/p52, p105/p50 and cRel shown as in "a". (d) p-Erk and total Erk shown as in "a".

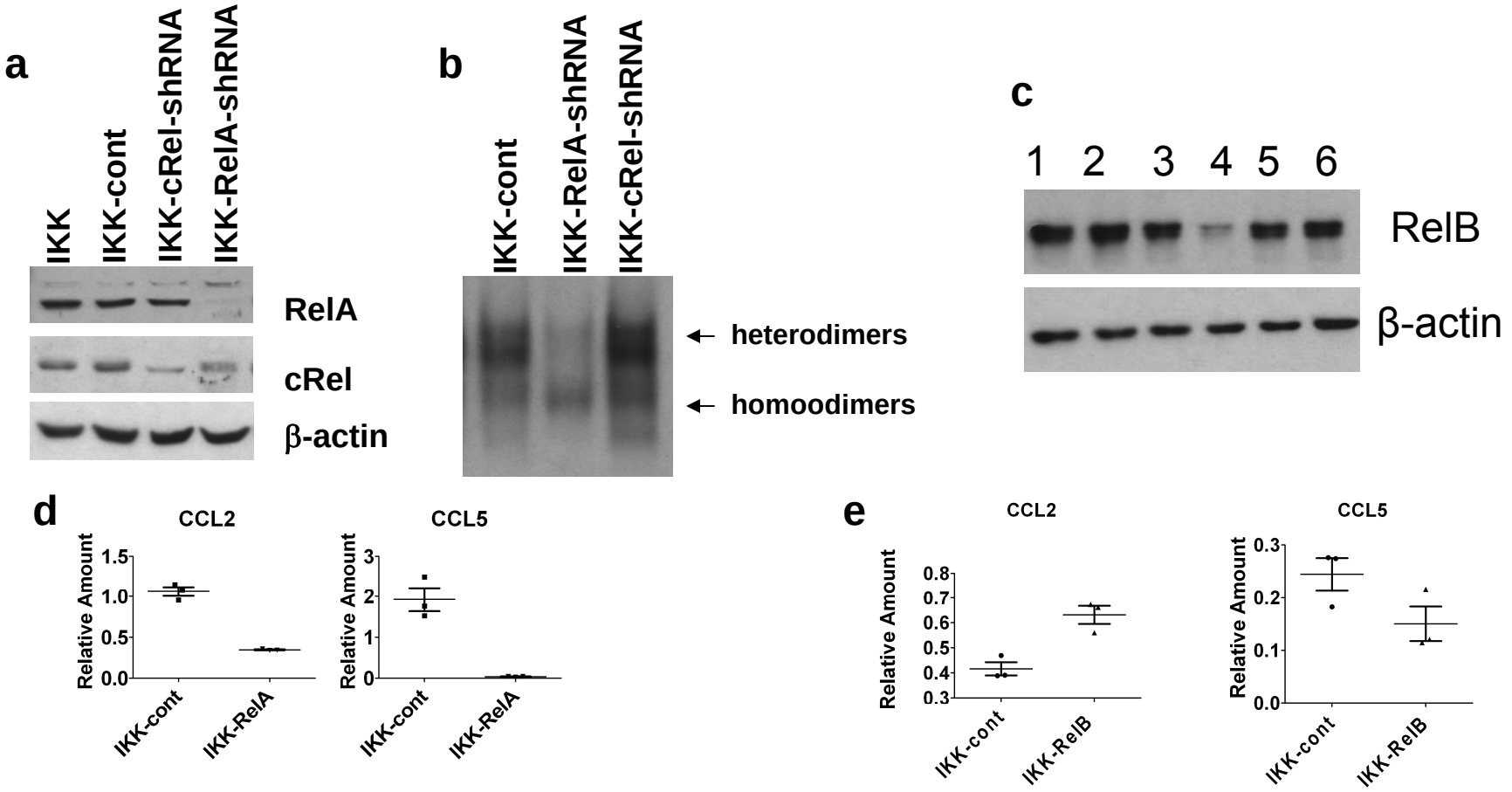

Supplemental Figure 8. (a) Western blot showing RelA and cRel levels in whole cell lysates after expression of control, RelA or cRel shRNA. (b) EMSA showing nuclear levels of NF-κB heterodimer and homodimer binding in LLC-OVA-IKK following expression of control, RelA or cRel shRNA. (c) RelB expression in LLC-OVA-IKK (lane 1), cells infected with control pLKO (lane 2) or different RelB specific shRNA (lanes 3-6). (d) CCL2 and CCL5 expression determined by RT-PCR after RelA shRNA expression in LLC-OVA IKK cells. (e) LLC-OVA-IKK cells expressing RelB shRNA in lane 4 of "c". RT-PCR expression of CCL2 and CCL5 is shown. Results are representative of at least two independent experiments.

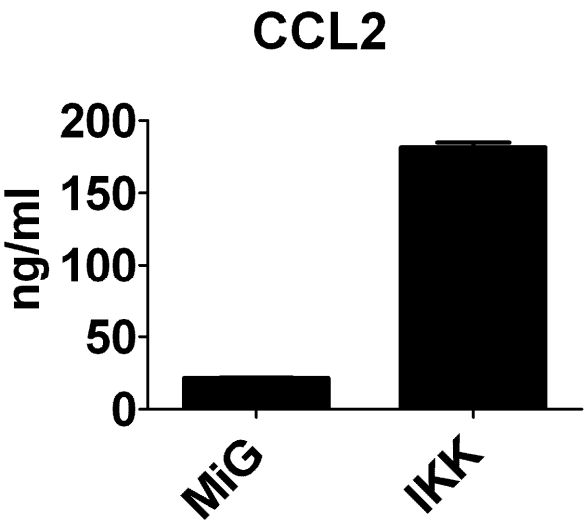

Supplemental Figure 9. LLC-OVA-MiG and LLC-OVA-IKK supernatants were collected 24h after plating and the amount of secreted CCL2 was determined by ELISA.

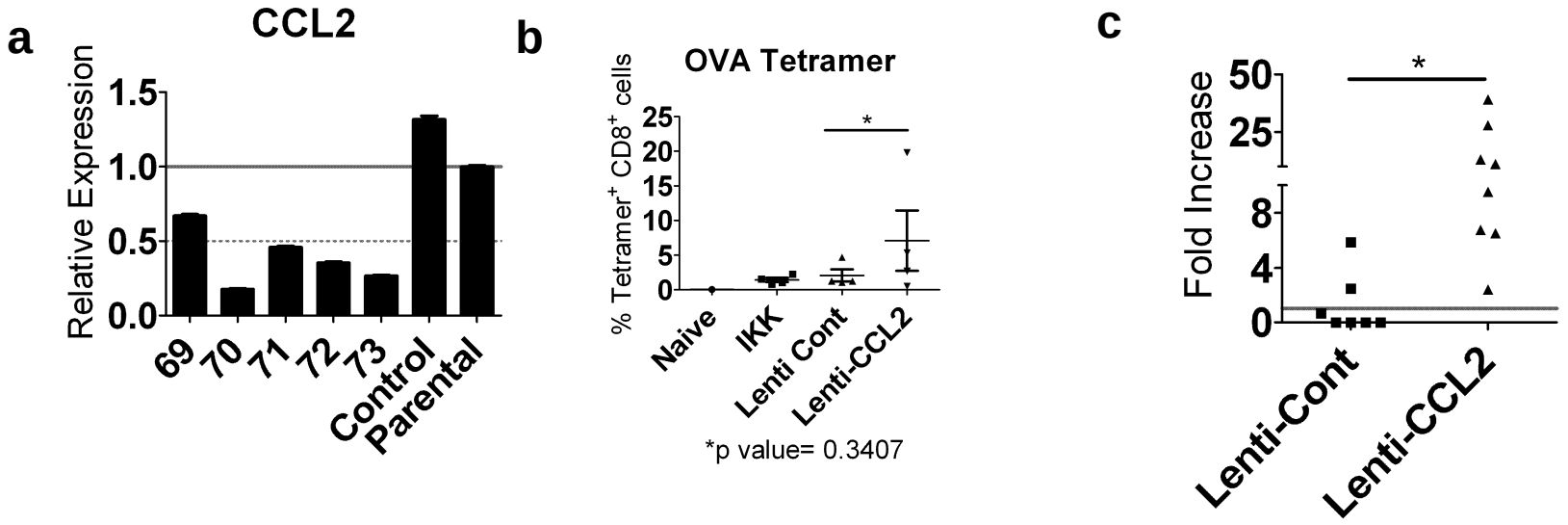

Supplemental Figure 10. Impact of CCL2 knock-down (KD) on tumor growth and anti-tumor immune response. (a) ELISA showing knock-down of CCL2 by lentiviral shRNA transduction in LLC-OVA-IKK cells relative to parental un-transduced LLC-OVA-IKK cells or control lentivurs infected cells. Samples were run in triplicate and reported as mean +/- SEM. shRNA "70" was used in studies described here. (b) Tetramer analysis of peripheral blood on day 10 from naïve mice or mice receiving LLC-OVA-IKK alone, transduced with lentiviral control, or CCL2 shRNA s.c. Each point represents a single mouse. Student's T test was performed to compare tetramer positive CD8 T cells between mice receiving LLC-OVA-IKK-lenti control and those receiving LLC-OVA-IKK-CCL2 KD tumors.(c) C57Bl/6 mice received s.c.LLC-OVA-IKK-lenti control or LLC-OVA-IKK-CCL2 KD and tumor growth was monitored. Relative fold increase in tumor volume in mice at D21 post-inoculation compared to D4 post-inoculation. Combined results from 2 independent experiments are shown. Each point represents tumor growth from a single mouse. The difference in tumor numbers showing growth in the two groups was significant, p value=0.007, Fisher's Exact Test.

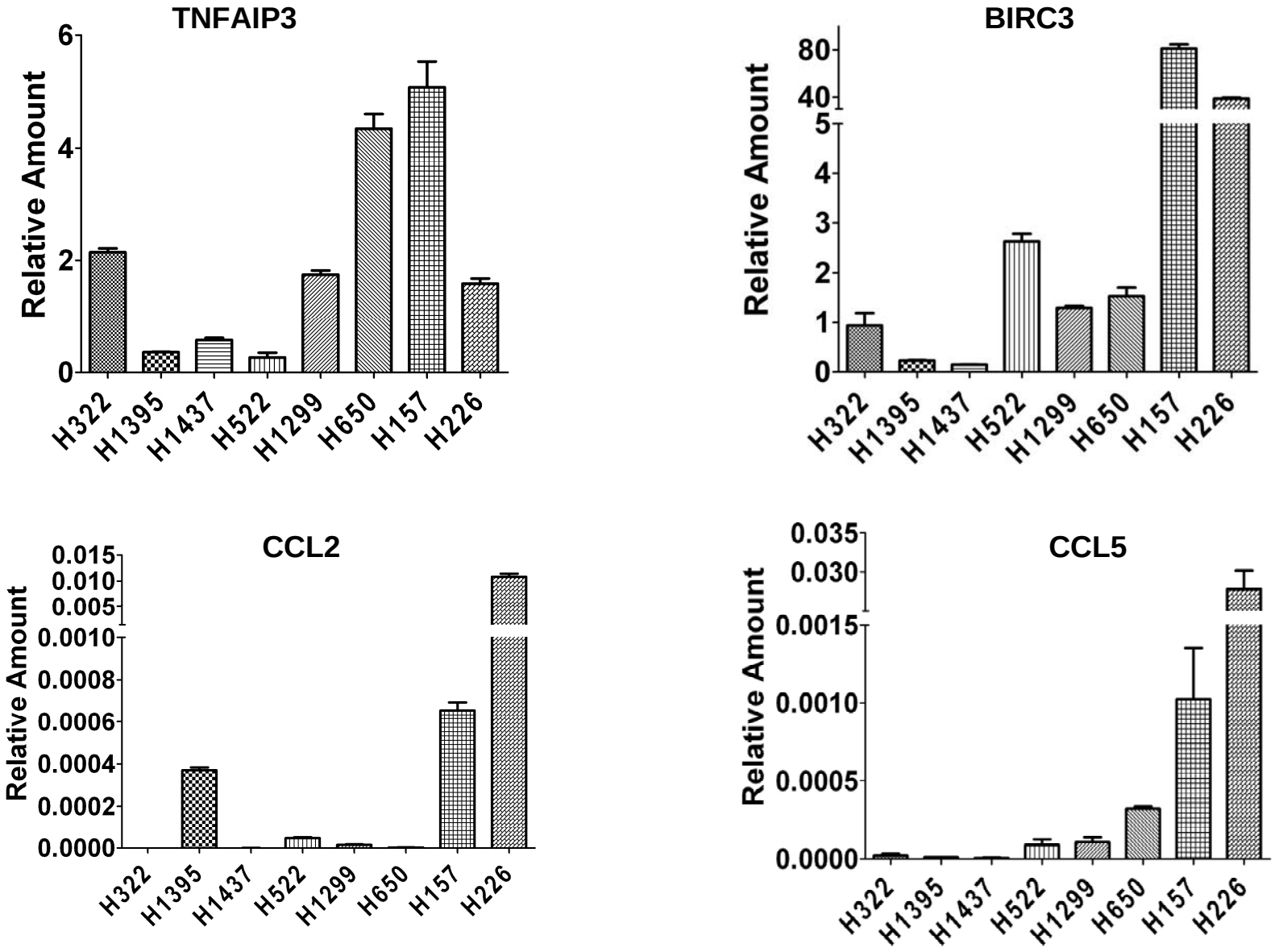

Supplemental Figure 11. Determination of mRNA expression of indicated NF-κB target genes in low NF-κB signature (H322, H1395, H1437, H522) and high NF-κB signature (H1299, H650, H157, H226) cells. Relative expression is shown after normalizing to 18s rRNA levels. Samples were run in triplicate and reported as average +/- SEM.

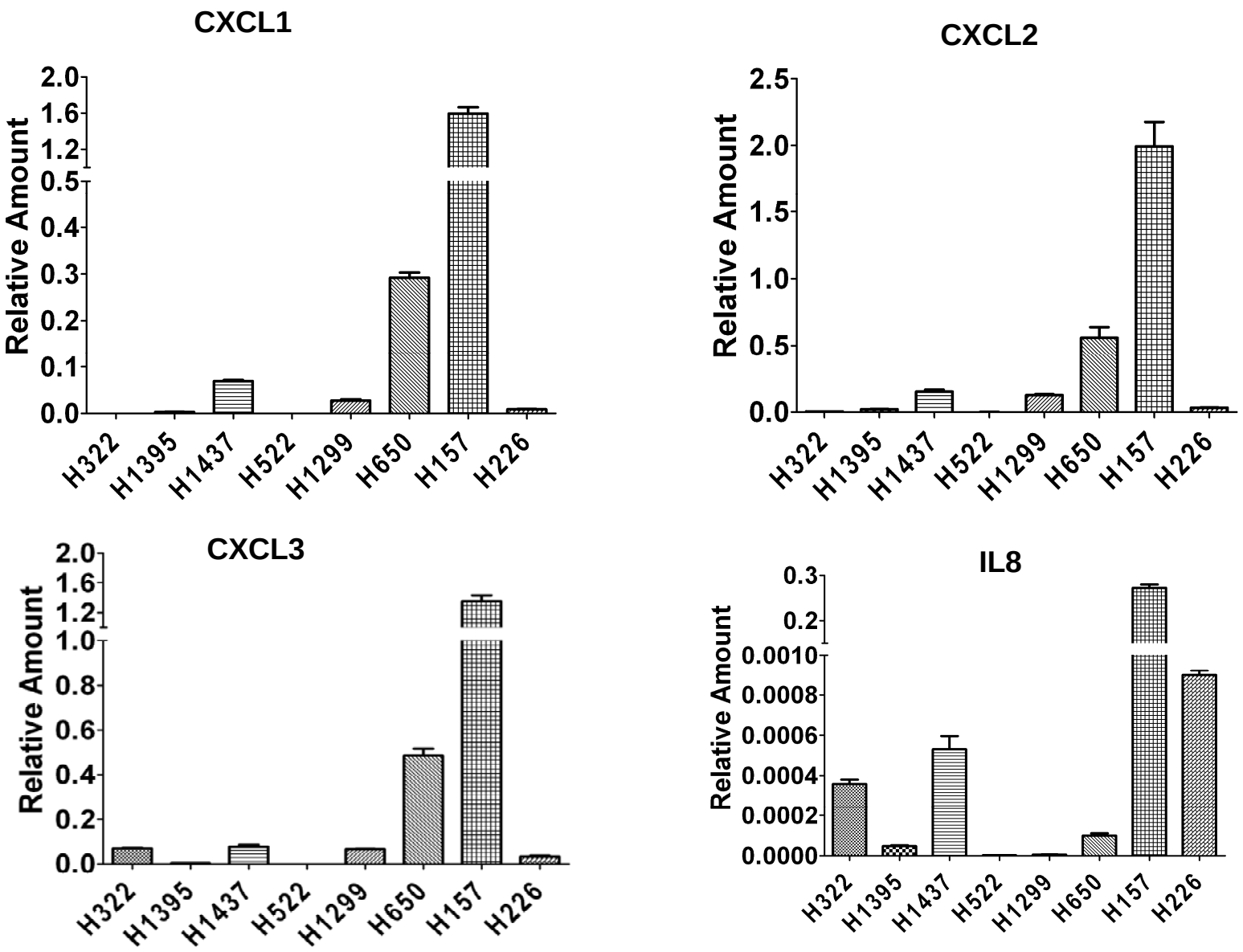

Supplemental Figure 11. Determination of mRNA expression of indicated NF-κB target genes in low NF-κB signature (H322, H1395, H1437, H522) and high NF-κB signature (H1299, H650, H157, H226) cells. Relative expression is shown after normalizing to 18s rRNA levels. Samples were run in triplicate and reported as average +/- SEM.

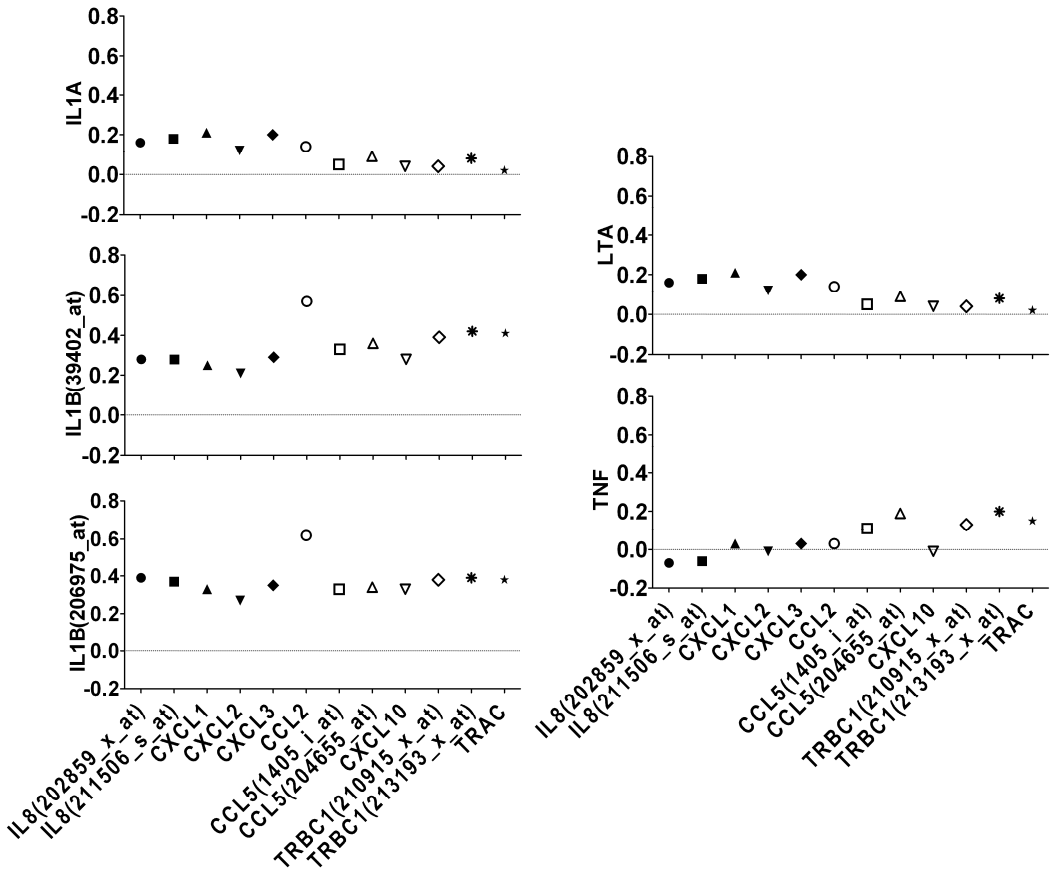

Supplemental Figure 12. Correlation of expression between genes in human lung adenocarcinoma. Correlation r-values of expression of different NF-κB activating cytokine genes (y-axis) with expression of different genes (x-axis). Gene name and Affymetrix probe set numbers for genes with 2 probe sets are shown.

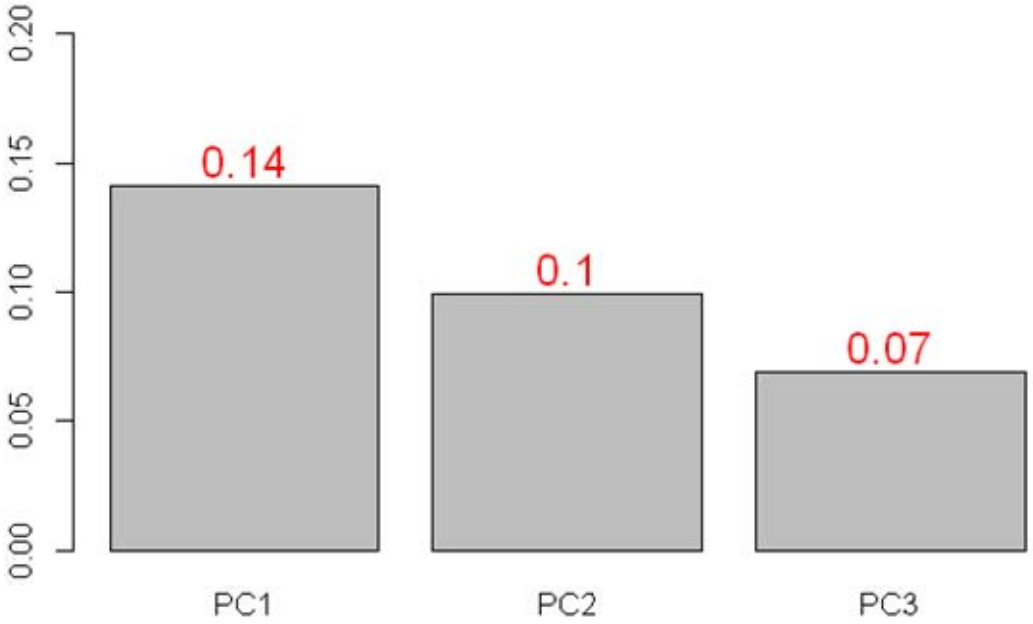

Supplemental Figure 13. The first 3 Principal Components (PC1-3) of the NF-κB signature are shown in the CMCLA dataset.

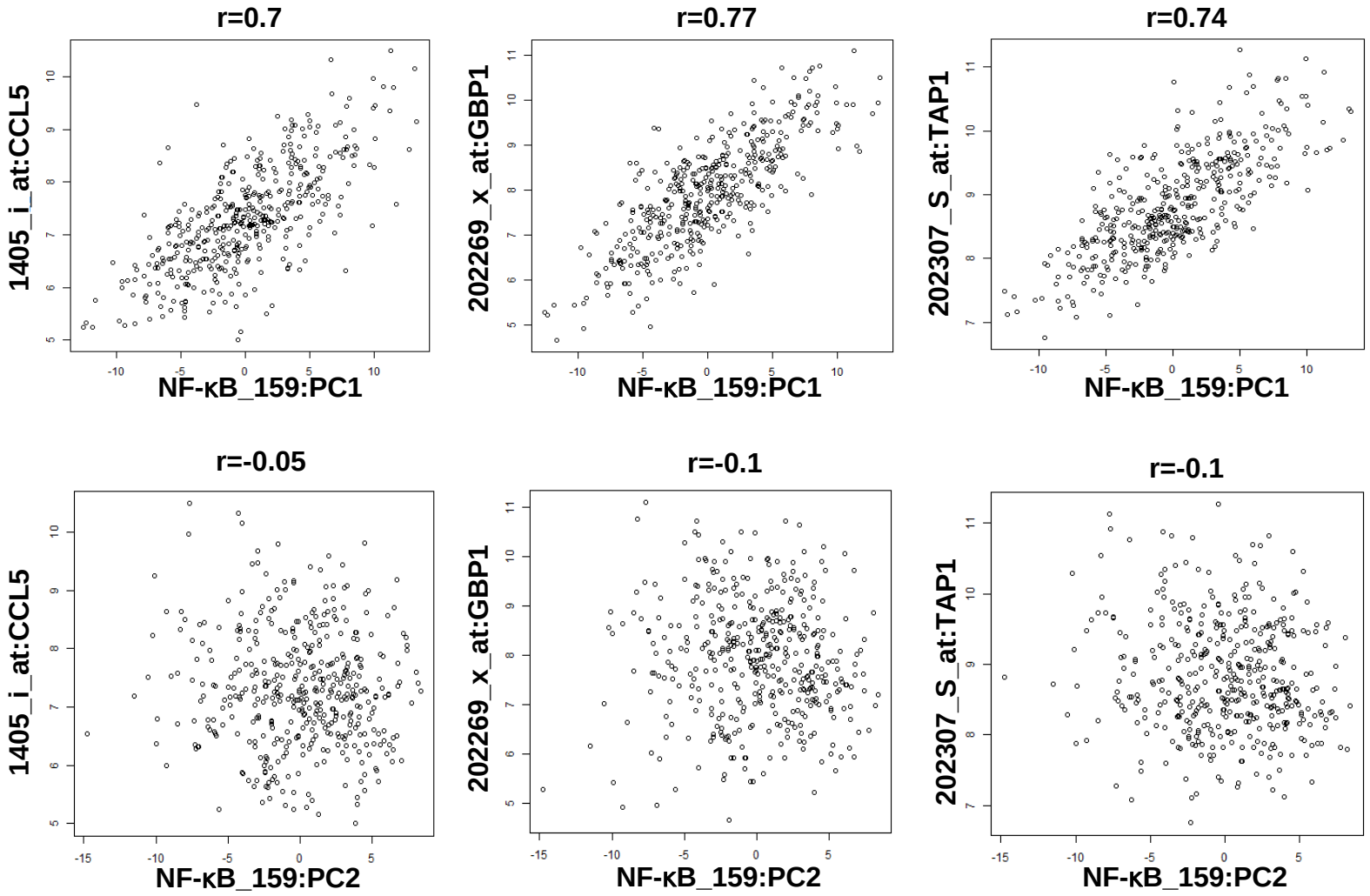

Supplemental Figure 14. Correlation of expression between NF-κB driver genes (y-axis) and PC1 (top panel) and PC2 (bottom panel) of the NF-κB signature 159 probesets (x-axis) in the CMCLA dataset. Correlation r-values, gene names and Affymetrix probe set ID are shown.

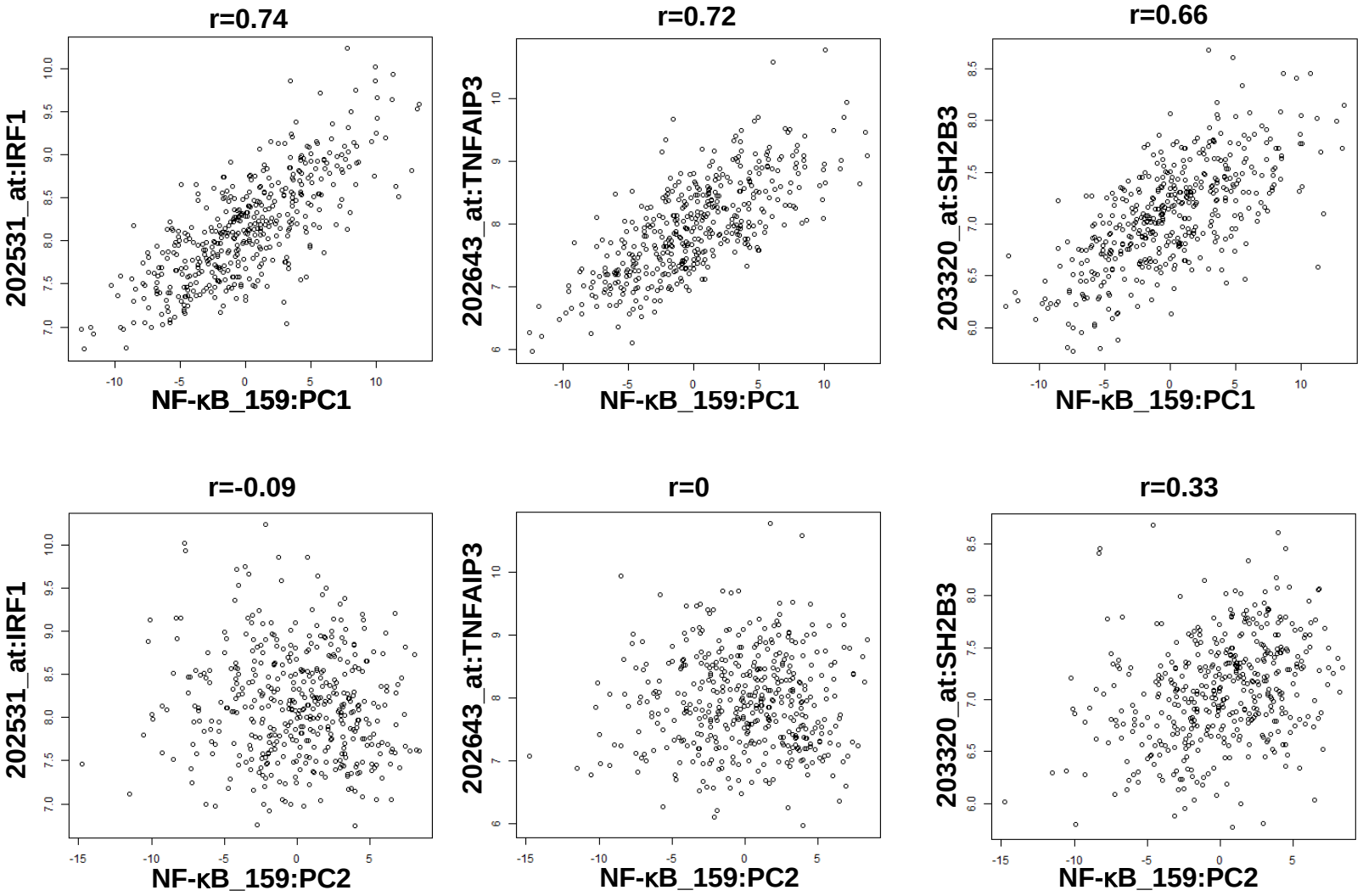

Supplemental Figure 14. Correlation of expression between NF-κB driver genes (y-axis) and PC1 (top panel) and PC2 (bottom panel) of the NF-κB signature 159 probesets (x-axis) in the CMCLA dataset. Correlation r-values, gene names and Affymetrix probe set ID are shown.

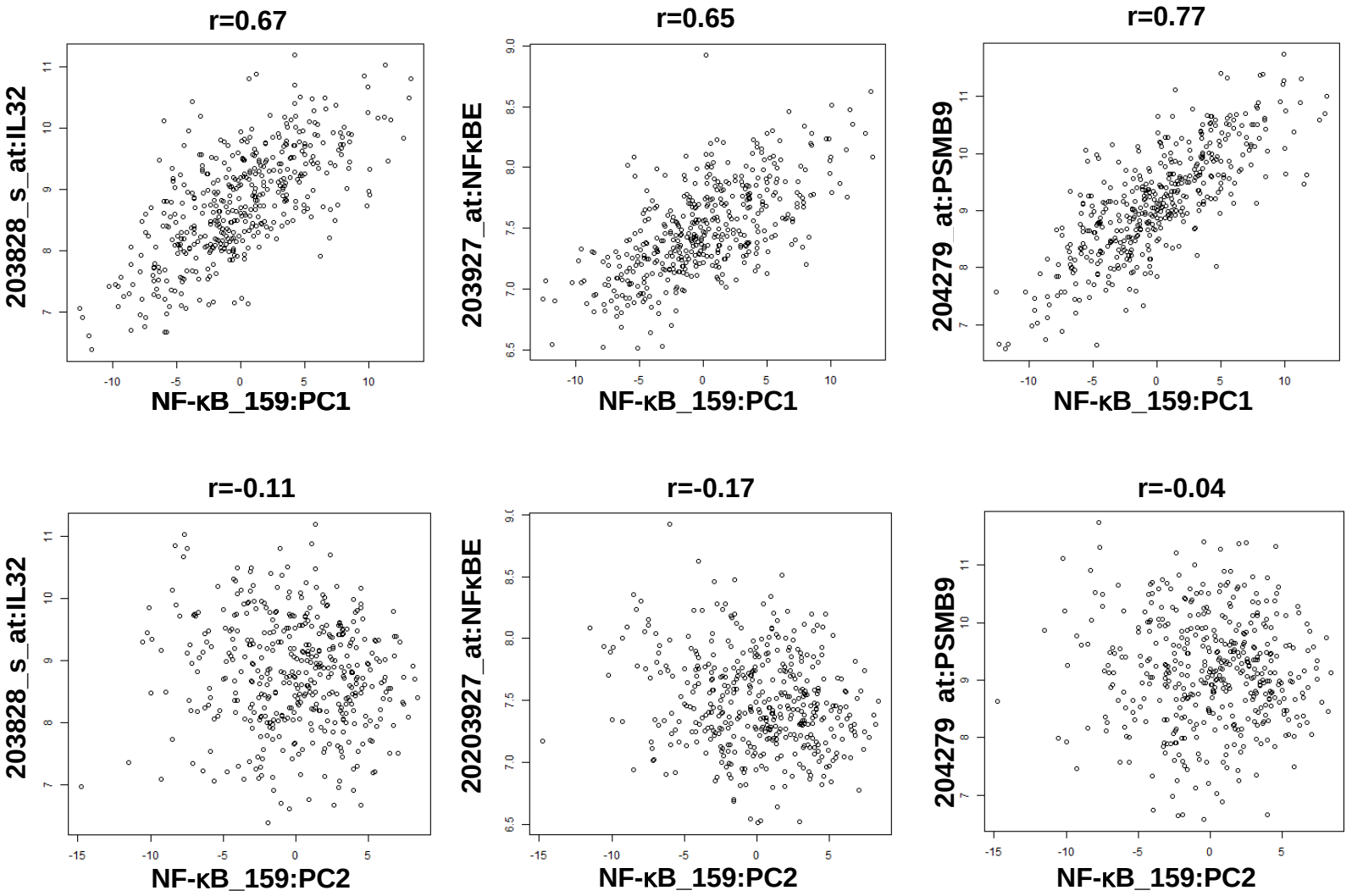

Supplemental Figure 14. Correlation of expression between NF-κB driver genes (y-axis) and PC1 (top panel) and PC2 (bottom panel) of the NF-κB signature 159 probesets (x-axis) in the CMCLA dataset. Correlation r-values, gene names and Affymetrix probe set ID are shown.

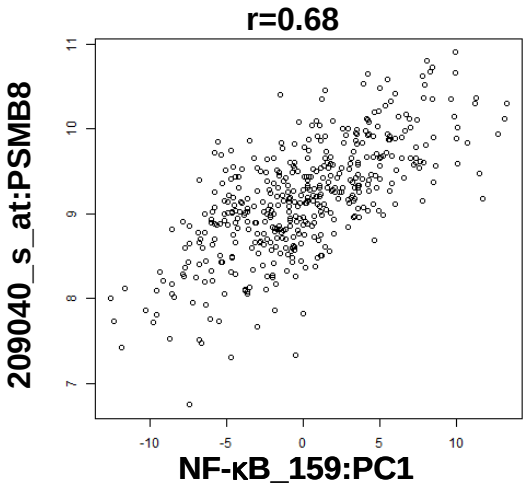

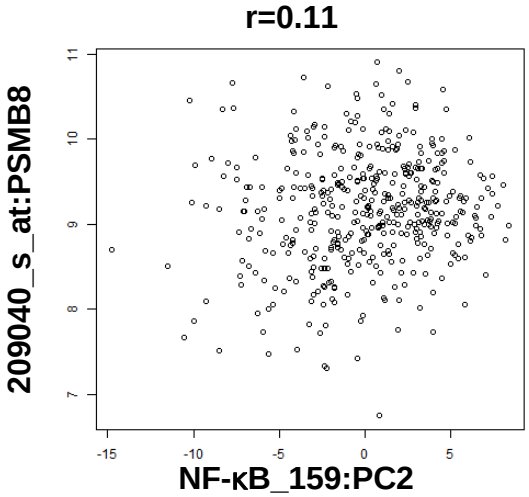

Supplemental Figure 14. Correlation of expression between NF-κB driver genes (y-axis) and PC1 (top panel) and PC2 (bottom panel) of the NF-κB signature 159 probesets (x-axis) in the CMCLA dataset. Correlation r-values, gene names and Affymetrix probe set ID are shown.

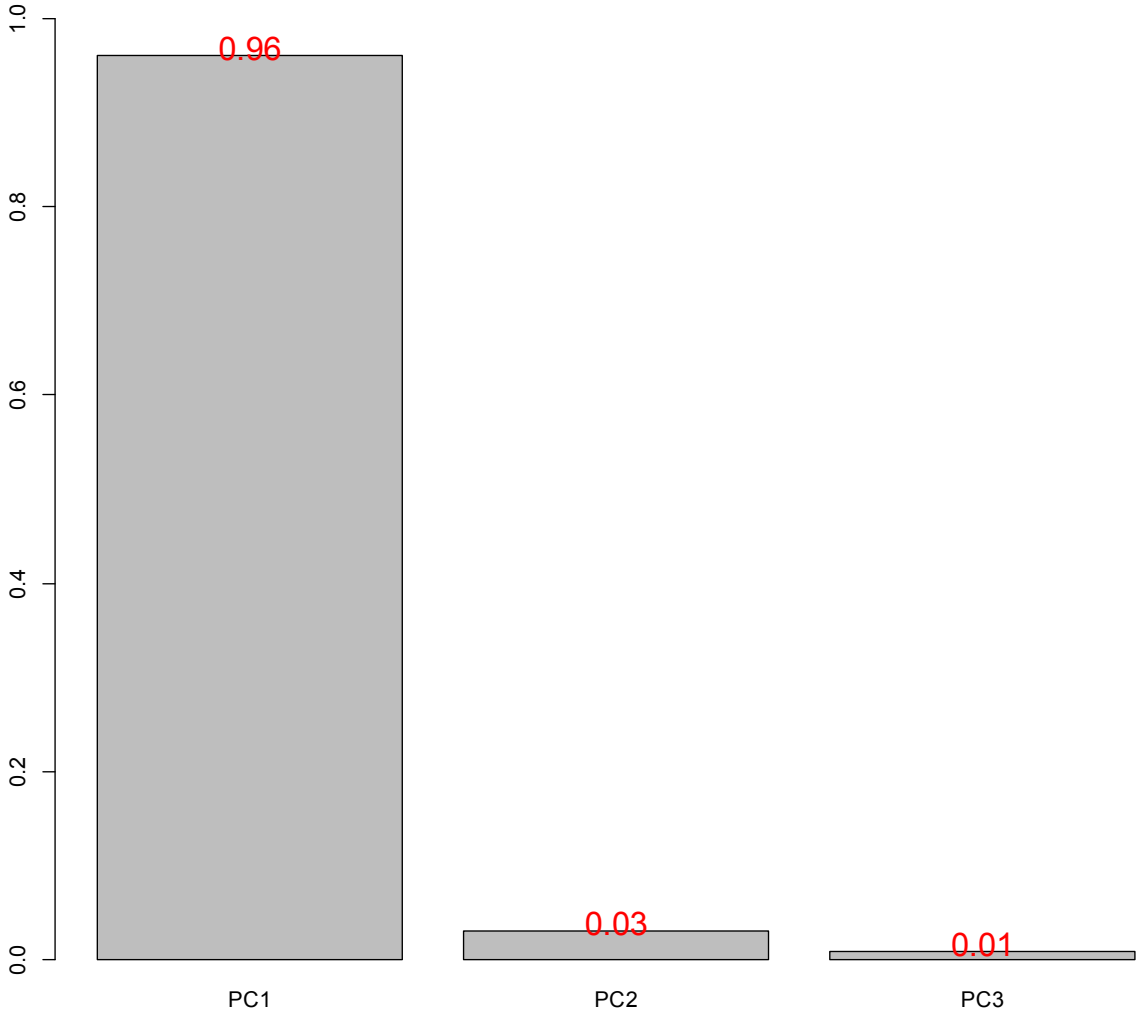

Supplemental Figure 15. The first 3 Principal Components (PC1-3) of the T cell receptor genes (TRAC and TRBC1) are shown in the CMCLA dataset.

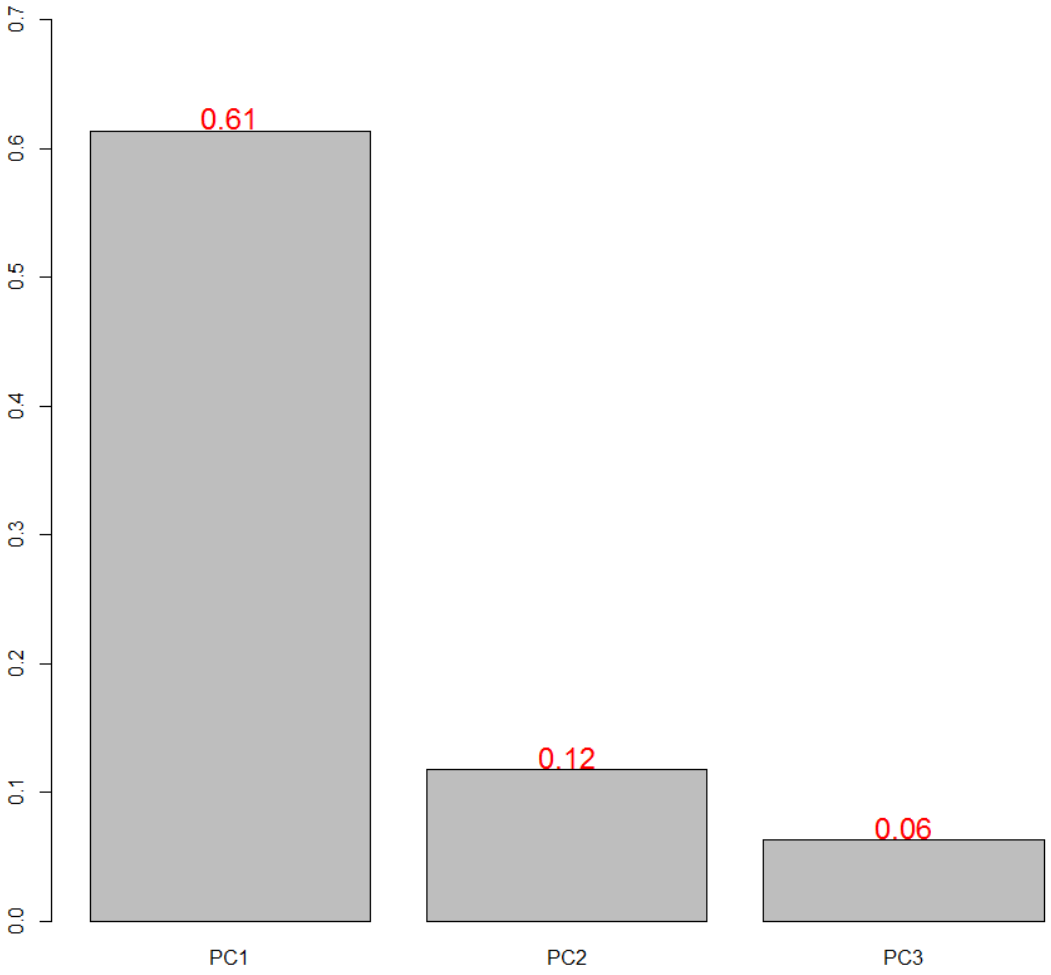

Supplemental Figure 16. The first 3 Principal Components (PC1-3) of the 10-gene NF-κB are shown in the CMCLA dataset.

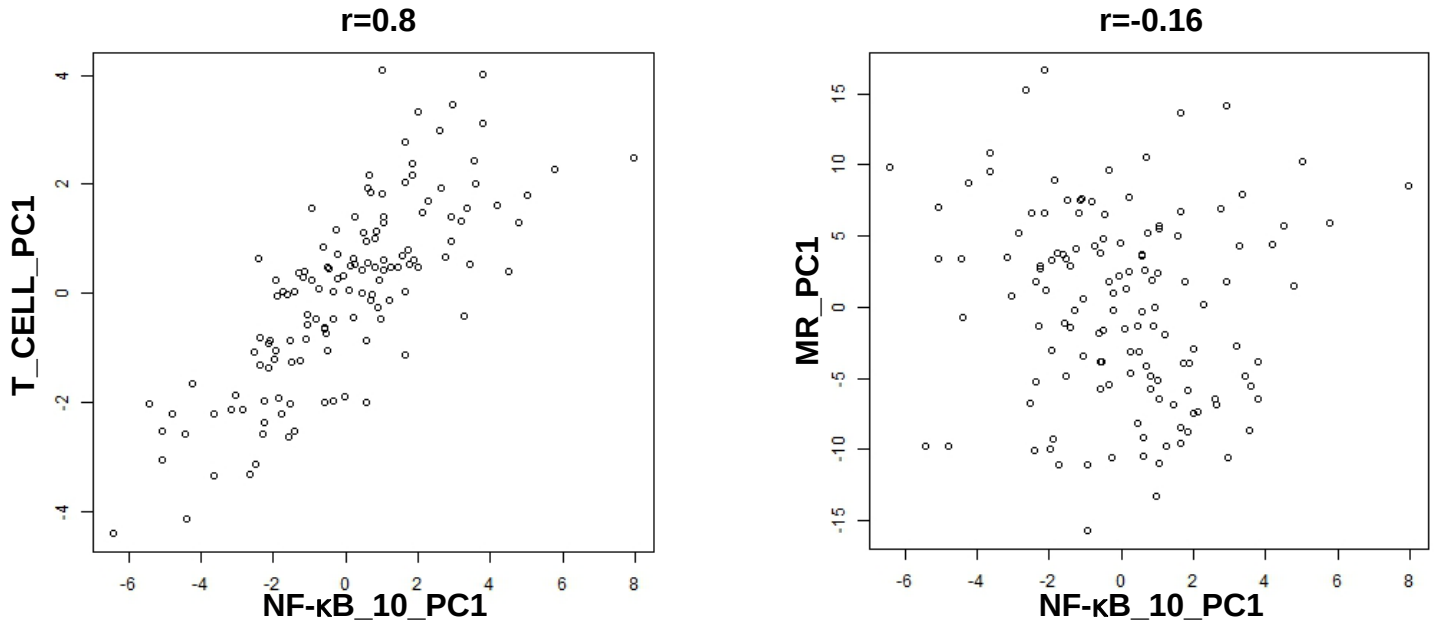

Supplemental Figure 17. Correlation of expression between the 10-gene NF-κB signature with T cell presence and the MR signature in the the GSE14814 dataset (n=133). Correlation r-values are shown.

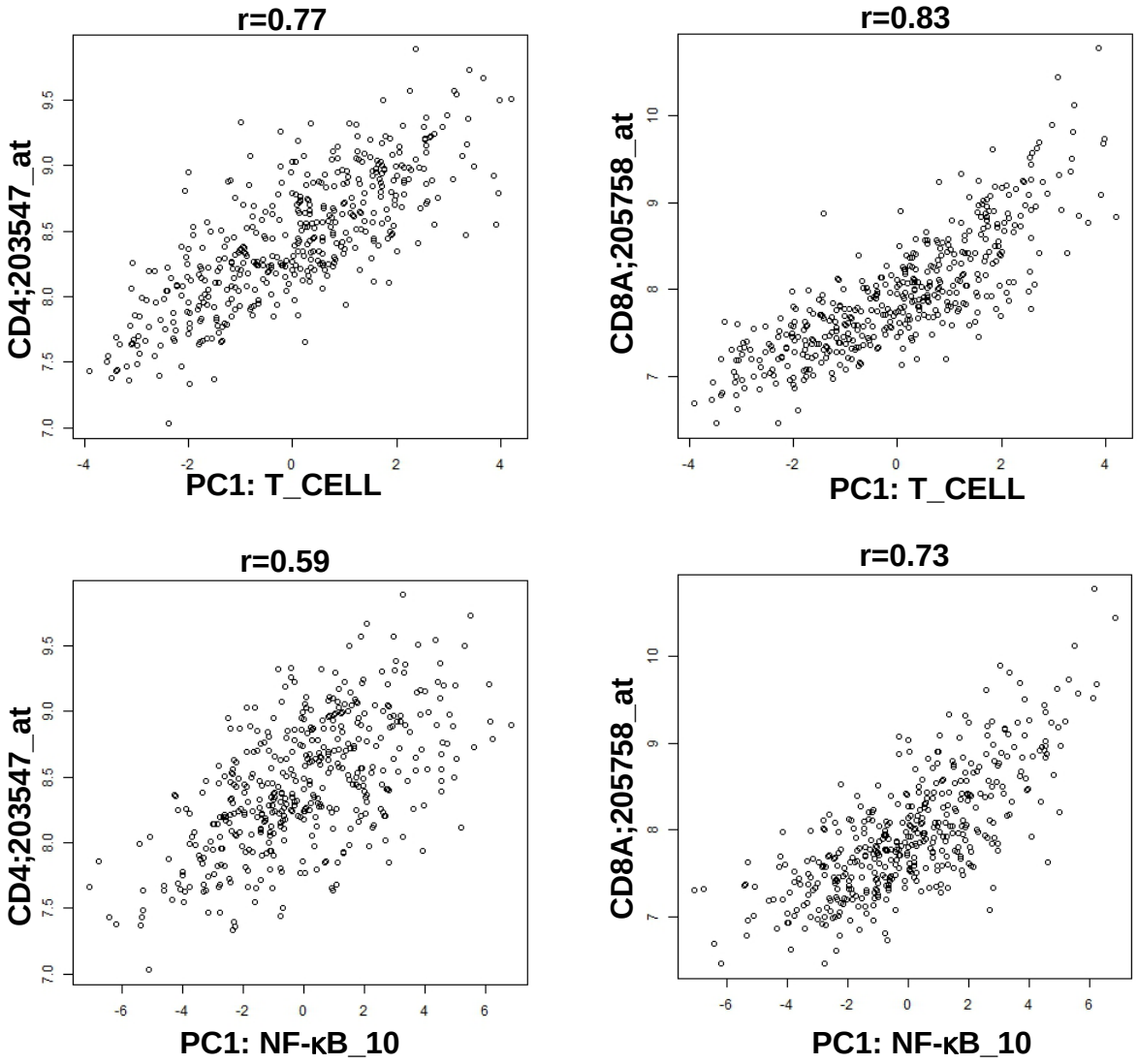

Supplemental Figure 18. Correlation between T cell presence and CD4 and CD8A expression (top panel). Correlation in expression between the 10-gene NF-κB signature and CD4 and CD8A expression (bottom panel). Data from the the CMCLA dataset is shown. Correlation r-values, gene names and Affymetrix probe set ID are shown.

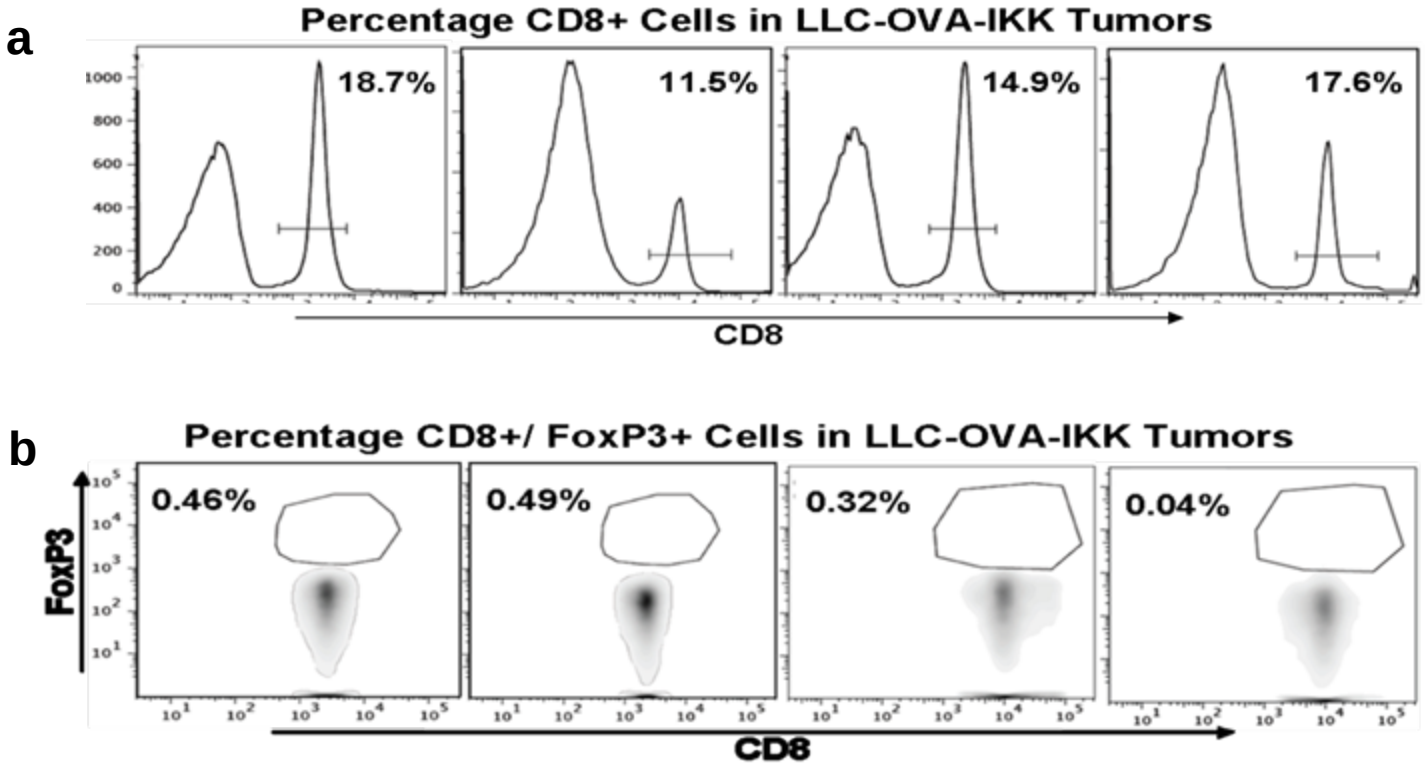

Supplemental Figure 19. Lymphocyte infiltration in LLC-OVA-IKK tumors. Mononuclear cells isolated from tumors 9 days post inoculation were analyzed for expression of CD8 (a). The percentage of CD8+ T cells is indicated. (b) CD8 and FoxP3 in mononuclear cells. The percentage of CD8+FoxP3+ T cells is indicated. Each graph represents an independent tumor.

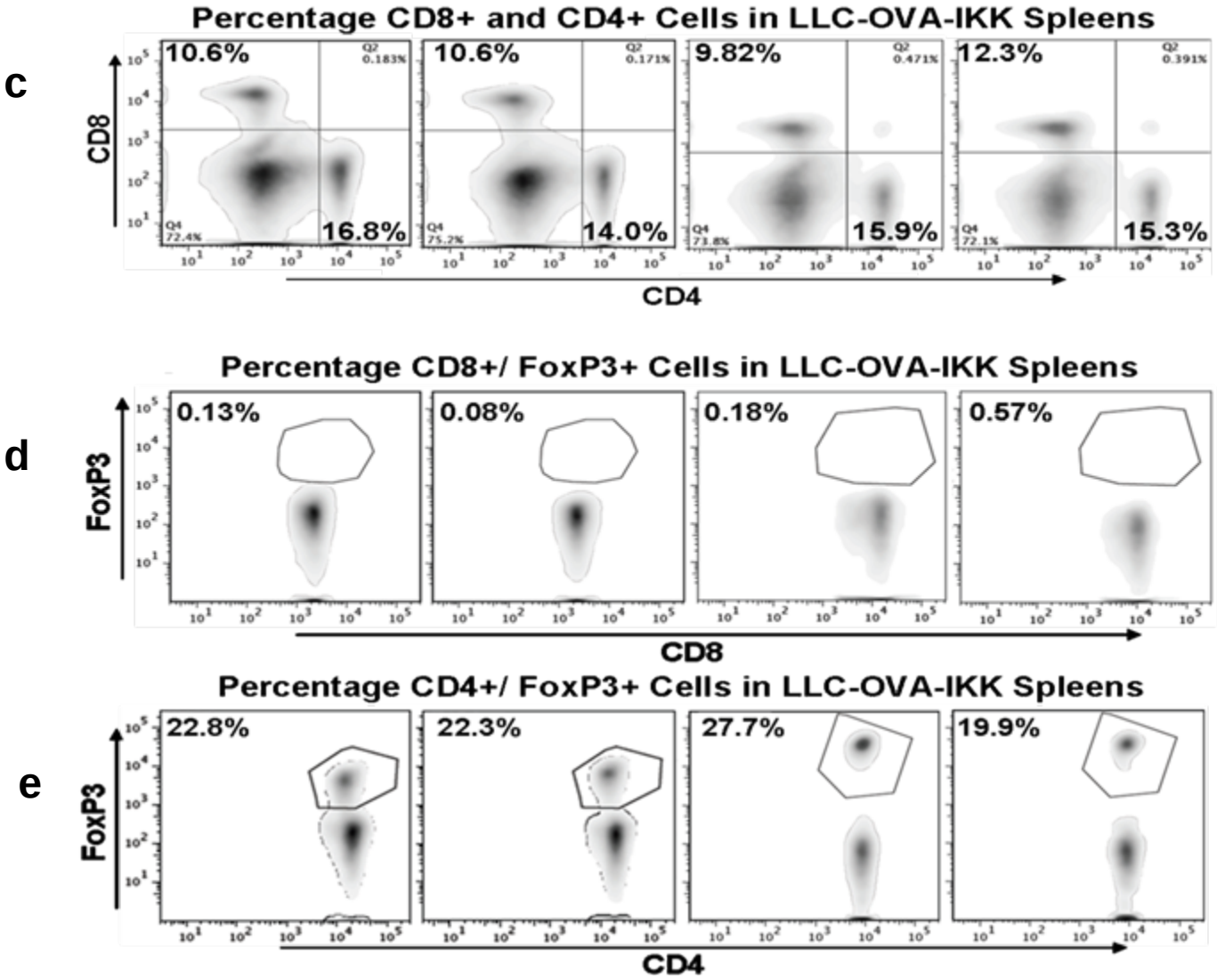

Supplemental Figure 19. Lymphocyte infiltration in LLC-OVA-IKK tumors. Mononuclear cells isolated from spleens of tumor bearing mice 9 days post inoculation were analyzed for expression of CD8, CD4 and FoxP3. (c) The percentage of CD8+FoxP3+ T cells after gating on CD8+ T cells. (e) The percentage of CD4+FoxP3+ T cells after gating on CD4+ T cells. Each graph represents an independent spleen.

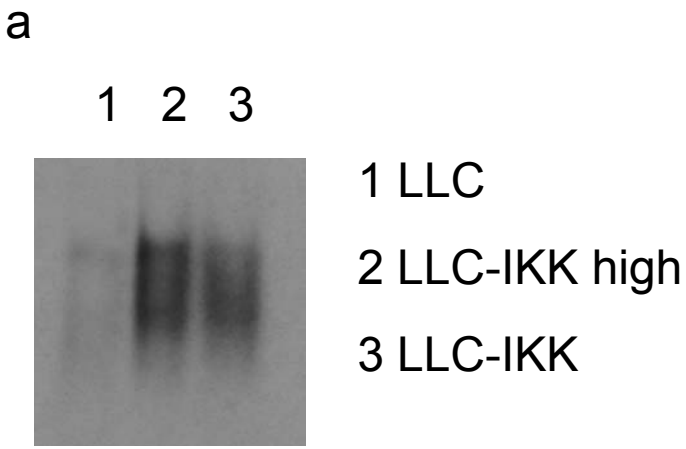

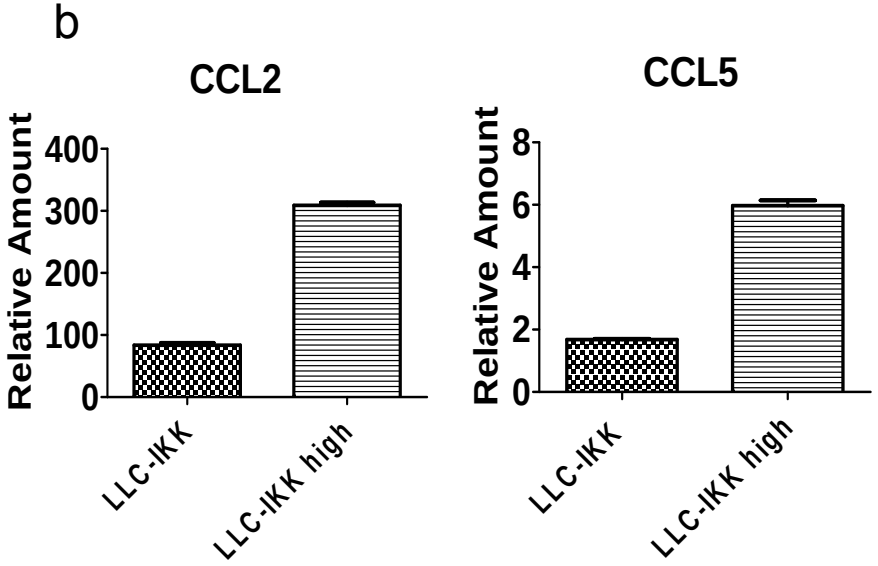

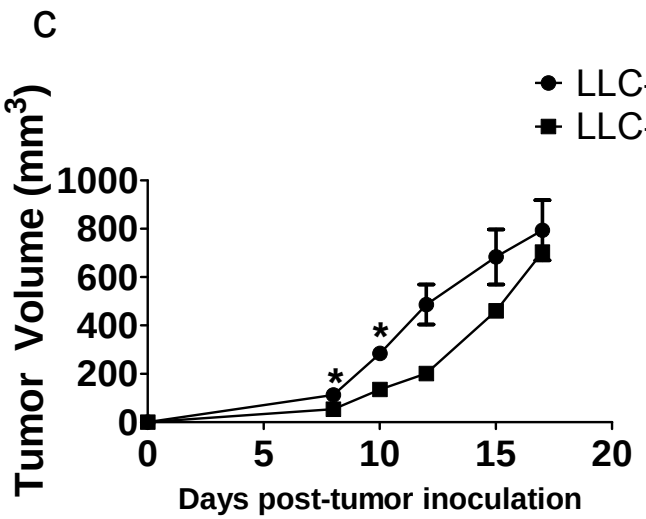

Supplemental Figure 20. Impact of IKKβ-induced NF-κB on tumor growth. (a) Electrophoretic mobility shift assay (EMSA) showing NF-κB nuclear levels in LLC, LLC-IKK and LLC-IKK-high. (b) RT-PCR showing CCL2 and CCL5 expression in LLC-IKK and LLC-IKK-high. Samples were run in triplicate and reported as average +/- SEM. (c) C57Bl/6 mice received s.c. LLC-IKK (n=3) and LLC-IKK-high (n=3) and tumor growth was monitored. Error bars represent SD. Significant difference in growth were observed at early time points (Day 10, p=0.0003, t test) but not at later time points (Day 17, p=0.6449, t test).

a

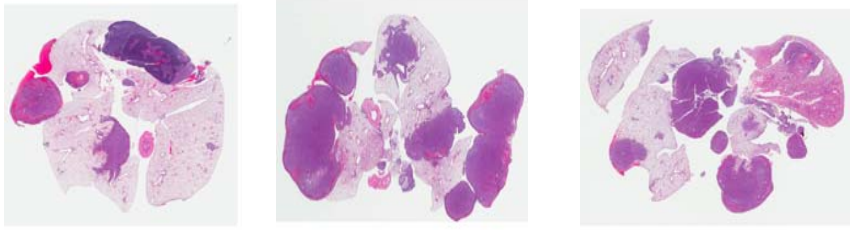

LLC-IKK

4mM

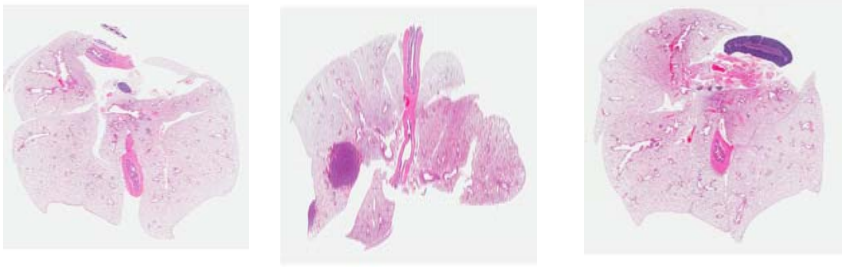

LLC-IKK High

4mM

c

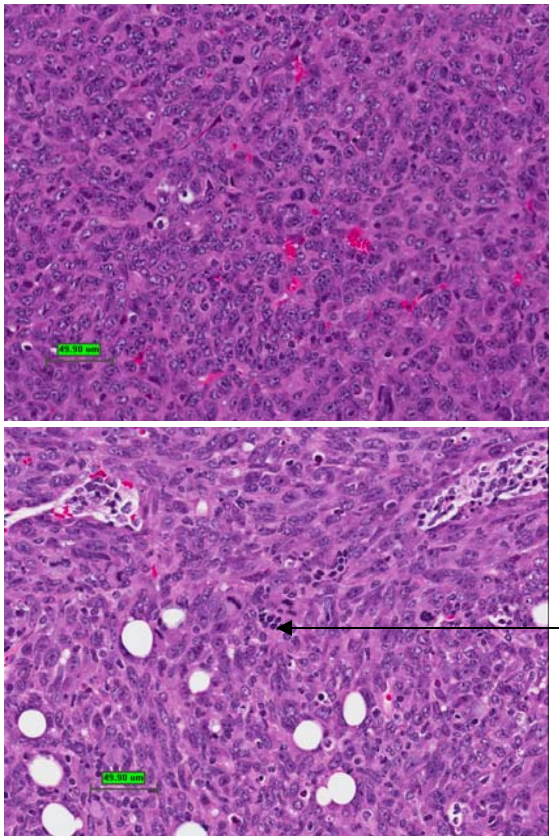

b

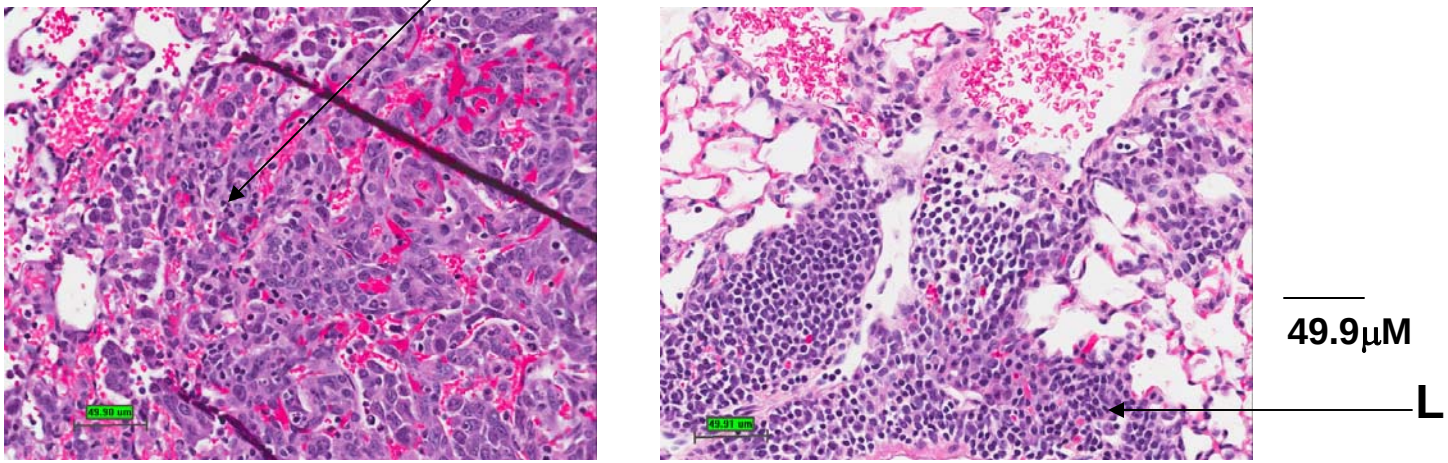

Supplemental Figure 21. Impact of IKKβ-induced NF-κB on tumor growth in a metastatic model of lung cancer. (a) H&E staining of lungs from mice 24 days after receiving i.v. LLC-IKK or LLC-IKK-high as indicated. (b) Larger LLC-IKK-high tumors showed lymphocytic infiltrates peripherally and within tumors (left) while smaller foci showed numerous lymphocytes with few remaining tumor cells (right). (c) LLC-IKK tumors showing presence of small numbers of lymphocytes (L).

Supplemental Materials

Microarray studies

Mouse LLC microarray: For microarray analysis the mRNA in 100 ng of total RNA was specifically converted to cDNA and then amplified and labeled with biotin using the Ambion Message Amp Premier RNA Amplification Kit (Life Technologies, Grand Island, NY) following the manufacturer's protocol. Affymetrix Mouse Genome 430 2.0 Arrays were used in these studies. Hybridization with the biotin-labeled RNA, staining, and scanning of the arrays following the prescribed procedure outlined in the Affymetrix technical manual. Results were analyzed using the MAS 5.0 algorithm. Genes were considered changed if they were identified as changed in the MAS 5.0 comparison analysis and there was a 2-fold difference in signal compared to the control condition.

Human NF-κB signature: Microarray analysis was initiated with 100 ng of total cellular RNA from each cell line. RNA was converted to cDNA and then amplified and labeled with biotin using the Ambion Message Amp Premier RNA Amplification Kit (Life Technologies, Grand Island, NY) following the manufacturer's protocol. The labeled RNA was hybridized to Affymetrix U133 Plus 2.0 microarrays and the staining, and scanning of the chips followed the prescribed procedure outlined in the Affymetrix technical manual. Results were analyzed using the MAS 5.0 algorithm with all treated samples compared to the corresponding control samples. In the preliminary analysis, genes were considered to be changed if they were identified as changed in the MAS 5 comparison analysis (p value 0.05) and there was a 1.4-fold difference in signal compared to the control. The initial lists were then considered together to identify genes that both activated in activating conditions and inhibited in inhibitory conditions across all 5 cell

lines. Genes meeting these criteria in at least 6 of the 10 experimental conditions were considered to be NF-κB responsive genes.

NF-κB cell-line classifier

The microarray data was obtained from GEO at NCBI and Array Express at EBI. It consists of 408 Affymetrix CEL files of 126 different lung cell lines. The scores were calculated based on this set of samples so the high and low are in reference to other cell lines within this group. The probesets that were used to classify the samples were the 240 probes originally identified in the 5 cell lines (i.e. NF-κB signature). The classifier was built and implemented as described (classifier H in supplemental materials and methods) (1). The decision thresholds were made based on the array of measures in the 408 lung CEL file data. The weighted voting classification of each sample scores each gene (probeset) based on where the signal value falls among all the samples in the group. If the probeset was positively correlated with the NF-KB signature (in the original 5 cell lines) then values in the lower third receive a score of -1, values in the middle third receive a 0, and values in the upper third receive a value of 1. If a gene was negatively correlated the values were reversed. The scores for all probesets were summed to provide the final classification score. The data sets used are listed below:

E-MTAB-37	Array Express
GSE10021	GEO
GSE10843	GEO
GSE13309	GEO
GSE14315	GEO
GSE14883	GEO
GSE15240	GEO
GSE16194	GEO
GSE17347	GEO
GSE18454	GEO
GSE21612	GEO
GSE4824	GEO

GSE5816	GEO
GSE6013	GEO
GSE7562	GEO
GSE8332	GEO

ELISA

Supernatant was collected from LLC-OVA-MiG cells and LLC-OVA-IKK cells after 24h of culture. Anti-CCL2 ELISA (Ready-SET-Go® kit from eBioscience (San Diego, CA) was performed to measure CCL2 production and secretion in cells and to confirm CCL2 knockdown according to the manufacturer's instructions.

Western blotting, electrophoretic mobility shift assays (EMSA) and shRNA knockdown

Protein lysates were prepared from whole cell or cytoplasmic and nuclear extracts and Western blots were performed as described (2). Antibodies were p-ERK/ERK (Cell Signaling, Danvers, MA), RelB sc-226x, p-RelA sc-33020, RelA sc-372X, p105/p50 sc-7178, cRel sc-70 were all from Santa Cruz Biotechnology (Santa Cruz, CA). p100 antibody was kindly provided by Dr. Nancy Rice (NIH), EMSA was performed as previously described (2). Mouse-specific RelA and cRel shRNA vectors were obtained from Addgene and have been previously described (3). RelB shRNA vectors were obtained from Open Biosystems.

Analysis of tumor infiltrating T cells

Spleens and tumors were obtained from mice on D9 post tumor inoculation and mechanically digested through cell strainers (40micron). The tumors were incubated with Collagenase D Buffer (Roche) (2mg/mL final solution) for 30min at 37˚C. All samples were resuspended in PBS and an equal volume of LSM (MSbio) was underlayed. Cells were centrifuged for 30min at

400Xg and the mononuclear interface was isolated. Cells were washed 2X in FACS Buffer, Fc blocked for 5min at RT, then cell surface staining was performed for 30min at 4˚C. Cells were next stained for intracellular FoxP3 as per ebioscience kit protocol. Briefly, cells were washed 2X in FACS Buffer, and then fixed for 30min at 4˚C. Next, cells were washed 2X in Perm Buffer and FoxP3 staining was performed for 30min at 4˚C. Cells were then washed once in Perm Buffer, and then resuspended in FACS Buffer. Data was collected on the LSRII (BD) and analyzed with FlowJo 7.65.

Supplemental Table 1. Microarray analysis of LLC-OVA-MiG compared to LLC-OVA-IKK cells. Genes shown were increased or decreased over 2-fold in LLC-OVA-IKK cells compared to LLC-OVA-MiG cells by Microarray. Genes are listed in order of decreasing fold-induction. Genes identified by multiple probesets are listed for each probeset and probesets lacking gene names are not included. The up-regulated, down-regulated and chemokines genes are shown.

Supplemental Table 2. NF-κB signature probeset list with indicated up-regulated and down-regulated probesets. Also shown are gene symbols (when known) and Genebank ID.

Supplemental Table 3. NF-κB signature score was determined using a classifier (S. Methods) in human lung cancer cell line data. Cell lines used are highlighted (H226, H157, H1299, H650, H322, H1395, H522, H1437), many of which were sampled multiple times.

Supplemental Table 4. NF-κB signature 159 probesets and gene symbols are indicated, when available, that were used for determining NF-κB signature activity in the CMCLA dataset.

References

1. Shedden, K., Taylor, J.M., Enkemann, S.A., Tsao, M.S., Yeatman, T.J., Gerald, W.L., Eschrich, S., Jurisica, I., Giordano, T.J., Misek, D.E., et al. 2008. Gene expression-based survival prediction in lung adenocarcinoma: a multi-site, blinded validation study. *Nat Med* 14:822-827.
2. Beg, A.A., Finco, T.S., Nantermet, P.V., and Baldwin, A.S. 1993. Tumor necrosis factor and interleukin-1 lead to phosphorylation and loss of IκB: a mechanism for NF-κB activation. *Mol. Cell Biol.* 13:3301-3310.
3. Meylan, E., Dooley, A.L., Feldser, D.M., Shen, L., Turk, E., Ouyang, C., and Jacks, T. 2009. Requirement for NF-kappaB signalling in a mouse model of lung adenocarcinoma. *Nature* 462:104-107.